

FLEXURAL STRENGTH OF IMPROVED LONGITUDINAL JOINT DETAILS IN GFRP-REINFORCED PRECAST DECKED BULB-TEE BRIDGE GIRDERS

Imad Eldin Khalafalla, M.A.Sc., Civil Engineering Department, Ryerson University, Toronto, Canada

Khaled Sennah, Ph.D., P.E., PCI Member, Civil Engineering Department, Ryerson University, Toronto, Canada

ABSTRACT

The use of glass fiber reinforced polymer (GFRP) bars to reinforce the bridge deck slabs as well as precast bridge deck slab joints in prefabricated bridge bulb-tee pre-tensioned girders is investigated experimentally. Four precast slab joint details were developed incorporating straight and headed ends GFRP bars embedded in a closure strip filled with non-shrink cement grout or ultra-high performance concrete (UHPC). Four actual-size specimens were cast representing the proposed joint details. In addition, other two control cast-in-place specimens were cast, namely: steel-reinforced specimen and GFRP-reinforced specimen. Results show the cast-in-place deck slab reinforced with GFRP reinforcement ratio specified by Canadian Highway Bridge Design Code (CHBDC) is as good as a similar slab reinforced with CHBDC-specified reinforcing-steel ratio. In addition, the closure strip filled with UHPC showed higher strength than other joint configurations considered in this study.

Keywords: GFRP-bars, Bridge deck slabs, Prefabricated girders, Closure strips, Non-shrink grout, Ultra-high performance concrete.

INTRODUCTION

The use of non-corrosive glass fiber reinforced polymer (GFRP) to replace reinforcing steel in deck slabs of precast bulb-tee girders is considered an innovative solution to eliminate the deterioration of deck slabs due to corrosion of steel. GFRP reinforcing bars has many advantages over steel reinforcement such as non-corrosive nature, high tensile strength in the direction of the fiber and light weight. Prefabricated bridge system made of deck bulb-tee (DBT) girders, shown in Fig. 1, can be an attractive choice for accelerating bridge replacement. In this system, the concrete deck slab is cast with the prestressed girder in a controlled environment at the fabrication facility and then transported to the bridge site. This system requires that the longitudinal deck joints be provided to make it continuous for live load distribution. Prefabricated elements can be quickly assembled and could reduce design efforts, reduce the impact on the environment in the vicinity of the site, minimize lane closure time and inconvenience to the traveling public. The Canadian Highway Bridge Design Code, CHBDC¹, and AASHTO-LRFD Bridge Design Specifications² do not provide guidance to design prefabricated concrete girder/deck joints made with GFRP bars. Also, there is no enough information available in the literature to design such joints. Moreover, there were no test data available to give confidence to the design of such joints. In this paper, results from six full-scale bridge deck slab models are built and tested to-collapse to examine new developed connection details between precast slab elements incorporating GFRP bars. The following sections summarize the specimens' details, experimental test procedure and test results.

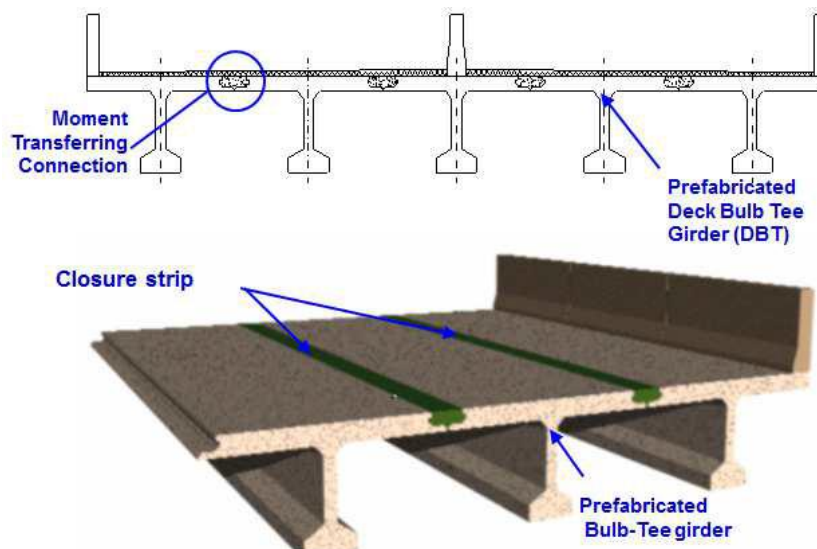


Fig. 1 Prefabricated bridge superstructure made of bulb-tee girder

NEW CONNECTION DETAILS

A prefabricated bridge system made of deck bulb-tee (DBT) girders is an attractive option for accelerating bridge construction. In this system, the concrete deck slab is cast with the

prestressed girder in a controlled environment at the fabrication facilities and then transported to the construction site. One of the main issues inherent in these prefabricated systems is the presence of cold joints created by the closure pours and their potential impact on the overall deck system behavior. In addition, it is important to develop effective connection details between the prefabricated elements to provide continuity of reinforcement in the closure strips so that load sharing between girders is not compromised. Few authors (Shah et al.^{3,4}; Au et al.^{5,6}) developed deck joints having closure strip widths ranging from 300 to 425 mm with projecting steel bars. This paper introduces glass fibre reinforced polymer (GFRP) bars as main reinforcement in the precast panels, projecting into the closure strip with and end head. FRPs, as non-corrodible materials, are considered as excellent alternative to reinforcing steel bars in bridge decks to overcome steel corrosion-related problems. Since it is less expensive than carbon and aramid FRPs, Glass FRP (GFRP) bars are more attractive to bridge deck applications. The GFRP bars used in this study have a tensile strength of 1188 MPa, compared to 400 MPa yield strength of reinforcing steel bars. The special “ribbed” surface profile of these bars, shown in Fig. 2, ensure optimal bond between concrete and the bar. Given the GFRP’s small transverse strength and relatively low modulus of elasticity, the shear strength of GFRP reinforced deck slab is lower than that for steel-reinforced deck slab. However, this issue is not important since shear strength in deck slabs is provided by concrete only. The favorable FRP characteristics include (i) high-strength-to-weight ratio; (ii) resistant to corrosion; (iii) durable (freeze and thaw resistance); and (iv) high chemical resistant⁷.

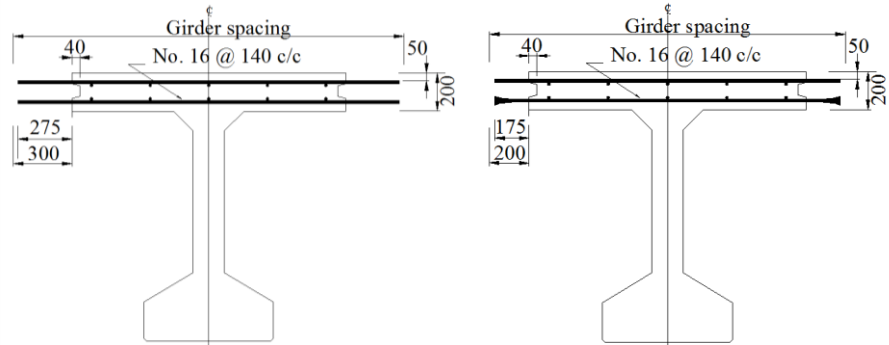
Until recently, the installation of GFRP bars was often hampered by the fact that bent bars have to be produced in the factory since GFRP bars cannot be bent at the site. Also, bent GFRP bars are much weaker than straight bars, due to the redirection and associated rearrangement of the fibres in the bent. As a result, number of bent GFRP bars is increased and even doubled at such locations where bar bents are required. The use of headed-end GFRP bars is intended to eliminate the expensive use of custom made bar bents. In this research on precast deck joints, GFRP bars with headed ends are introduced to reduce their development length into the joint, thus reducing the closure strip width. This GFRP bar headed end is made of a thermo-setting polymeric concrete with a compressive strength far greater than that of normal grade concrete. It is cast onto the end of the straight bar and hardened at elevated temperatures. The concrete mix of the bar head contains an alkali resistant Vinyl Ester resin, the same material used in the straight bars, and a mixture of fine aggregates. The maximum outer diameter of the head at its end is 2.5 times the diameter of the bar. The head of the 16 mm bar is approximately 100 mm long. It begins with a wide disk which transfers a large portion of the load from the bar into the concrete. Beyond this disk, the head tapers in five steps to the outer diameter of the blank bar. This geometry ensures optimal anchorage forces and minimal transverse splitting action in the vicinity of the head.

Four connection details with closure strip widths of 300, 200 and 125 mm, were proposed incorporating GFRP bars. Figure 3 shows schematic diagrams of the bulb-tee girders with projecting GFRP bars for two of these joints. The first proposed connection has 300 mm wide closure strip as shown in Fig. 4-a. In this connection the precast slab, both the top and bottom GFRP bars project into the joint with a 275-mm anchorage length. It is assumed that

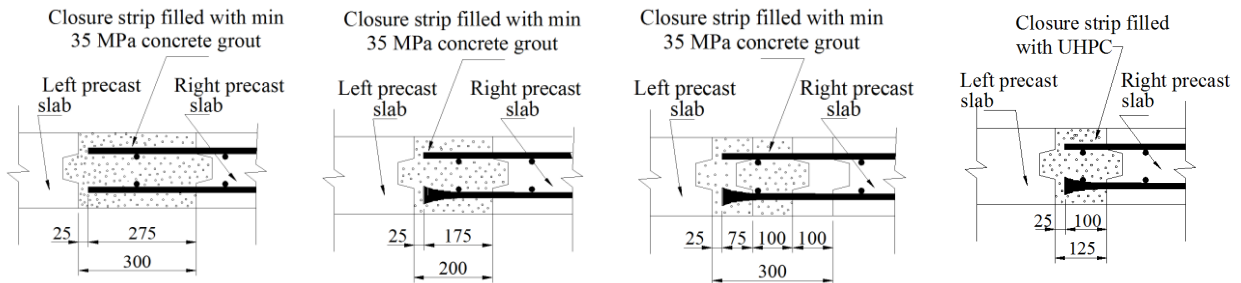
DBT girders will be aligned to provide 300 mm gap that can be filled using a minimum of 35-MPa cement grout. In bridge construction, Ontario Ministry of Transportation (MTO) adopts the standard 225 mm thick cast-in-place deck slab in Ontario bridges. This slab thickness incorporates 65 mm top concrete cover as recommended by CHBDC for reinforcing steel bars for protection against possible corrosion. However, with the use of non-corrosive FRP bars, the deck slab thickness can be reduced to 40 mm as specified in CHBDC with the use of FRP reinforcement. This makes the FRP-reinforced deck slab thickness 200 mm, thus reducing the material of the deck slab by about 12%. As a result, it is decided to conduct this research using 200 mm thickness for all slabs considered in this study.



Fig 2 Views of GFRP bars



(a) Straight-bar Joint (b) Headed bar joint
Fig. 3 Schematic diagrams of the bulb-tee girder and GFRP-bars



(a) Closure strip for S3; (b) Closure strip for S4; (c) Closure strip for S5; (d) Closure strip for S6
Fig. 4 Proposed closure strips

The second proposed connection detail between precast flanges of bulb-tee girders, shown in Fig. 4-b, has a 200-mm wide closure strip. The precast slab bottom GFRP bars project into the joint with headed end to provide a 175-mm anchorage length in the tension zone of the slab thickness, while the top transverse GFRP bars project into the joint with a 175-mm anchorage length in the compression zone of the joint. It is assumed that DBT girders will be aligned to provide 200 mm gap that can be filled using a minimum of 35-MPa cement grout. The third proposed connection has a 100 mm wide closure strip with staggered 100 mm wide trapezoidal-shaped (zigzagged-shaped) interlock between the precast flanges as shown in Fig. 4-c and in the plan of Fig. 6-c. In this connection, the precast slab bottom GFRP bars project into the joint with headed end to provide a 175 mm anchorage length in the tension

zone of the slab thickness, while the top transverse GFRP bars project into the joint with 175 mm anchorage length in the compression zone of the joint. It is assumed that DBT girders will be aligned to provide a 100 mm gap that can be filled using a minimum of 35-MPa cement grout. The interlocking shape of the joint shown in Fig. 4-c and in the plan of Fig. 6-c will provide a 175 mm total length of the headed bar into the joint.

The fourth proposed connection detail of 125 mm width is proposed as shown in Fig. 4-d. In this connection, the precast slab bottom GFRP bars project into the joint with headed end to provide a 100 mm anchorage length in the tension zone of the slab thickness, while the top GFRP bars project into the joint with 100 mm anchorage length in the compression zone of the joint. DBT girders will be aligned to provide a 125 mm gap that can be filled using ultra high-performance concrete (UHPC). It should be noted that each joint has 50-mm deep, 40-mm wide, trapezoidal shape shear key throughout the girders length. Also Fig. 4 shows projecting GFRP bars from one side of the joint only for clarity and the joint would consist of staggered projecting bars that would allow for ease of assembly in the bridge site.

EXPERIMENTAL PROGRAM

The experimental program included six full-scale deck slab specimens of 2500-mm length and 200-mm thick. A 600-mm slab width is considered for a slab strip. The 600-mm width is assumed oriented in the direction of traffic while the slab span represents the spacing between precast girders. As such, the main tension reinforcement in the tested specimens represents deck slab reinforcement normal to the girders shown in Fig. 1. It is understood that this slab configuration will provide conservative values for the flexural capacity at the mid-span of the slab since the wheel load will be distributed only over a 600 mm width. The span of the slab was taken 2000 mm with slab total length of 2500 mm to accommodate proper bars anchorage beyond the supporting points. The first deck slab specimen, S1, is formed of cast-in-place concrete reinforced with steel bars of 400 MPa yield strength. In this research, 10M reinforcing steel bars spaced at 200 mm *c/c* were used in all directions for the bottom and top layers representing the CHBDC-specified minimum steel reinforcement of 0.3% of the concrete area in each direction and each mesh. The second deck slab strip, S2, is similar to cast-in-place slab S1 but with straight GFRP bars. GFRP bars of 16-mm diameter, spaced at 140 mm *c/c*, were used as bottom tension reinforcement while the top main and transverse reinforcements were taken 12-mm GFRP bars spaced at 200 mm *c/c*. Transverse bottom reinforcement in the tested slab was provided by 16-mm diameter GFRP bars, spaced at 225 mm *c/c*. View of the reinforcement of slab S2 is shown in Fig. 5-a.

The third deck slab, S3, is similar to second slab S2 but considering the precast deck system shown in Fig. 1 and the precast flange-to-flange connection detail shown in Fig. 4-a. The amount and spacing of GFRP bars in the precast flanges were the same as those for the cast-in-place deck slab S2. Figure 5-b shows view of the GFRP bar layout in S3 slab formwork, while Fig. 6-a shows view of straight GFRP bars projecting into the closure strip of slab S3 before casting non-shrink grout. The fourth deck slab, S4, is identical to the joined precast slab S3, except that the joint width was reduced to 200 mm and the projecting bottom bars

into the closure strip were of headed ends as shown in Fig. 4-b. Figure 5-c shows view of the GFRP bar layout in S4 slab formwork, while Figure 6-b shows view of GFRP bars projecting into the closure strip of slab S4 before casting non-shrink grout. The fifth deck slab, S5, is formed of precast deck system shown in Fig. 1 and the precast flange-to-flange connection detail shown in Fig. 4-c.

A trapezoidal-shaped (zigzagged-shaped) interlock closure strip is introduced between the connecting flanges as shown in Fig. 4-c. Headed end GFRP bars of 16-mm diameter, spaced at 200 mm c/c, were used in the bottom tension side while the top main and transverse reinforcement was taken 12-mm diameter GFRP bars spaced at 200 mm c/c. The bottom transverse reinforcement was taken 16-mm diameter GFRP bars, spaced at 225 mm c/c. Figure 5-d shows view of the GFRP bar layout in S5 slab formwork, while Figure 6-c shows view of headed end GFRP bars projecting into the closure strip of slab S5 before casting non-shrink grout. The sixth deck slab, S6, is similar to the joined precast slab S4, except that the joint width was reduced from 200 to 125 mm to account for the increase in bond resistance of the GFRP bars embedded in ultra-high performance concrete (UHPC) rather than the ordinary cement grout used in slab S4. Figure 5-e shows view of the GFRP bar layout in S6 slab formwork, while Figure 6-d shows view of headed end GFRP bars projecting into the closure strip of slab S6 before casting UHPC. Table 1 summarizes the main variables of the tested slabs.



(a) Slab S2 (b) Slab S3 (c) Slab S4 (d) Slab S5 (e) Slab S6

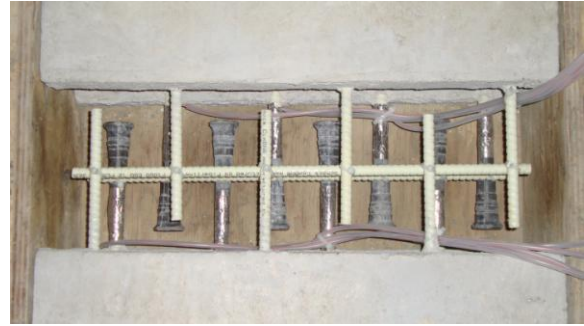
Fig. 5 Reinforcement Layout in Slab specimens

Concrete having a specified 28-day compressive strength of 35 MPa was used for both cast-in-place and precast deck slabs. Standard cylinders of 150-mm diameter and 300-mm height were cast concurrently with the casting of the deck slabs. An average of three cylinders were cast and stored close to the test samples to ensure the same curing conditions after casting. Non-shrink grout extended with 9.5-mm pea gravel was used for closure strips. The grout has a specified 3-day compressive strength of 31 MPa and 28-day strength of 59 MPa. Ultra-High-Performance Concrete (UHPC) having a 28-day specified strength of 100 MPa was used for closure strip. During the pouring of the grout/UHPC into the precast deck slab

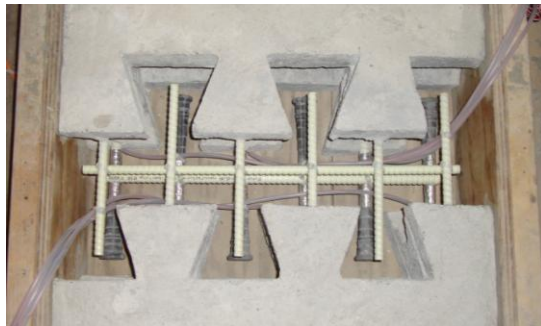
closure strips, standard cylinders of 100-mm diameter and 200-mm height were cast and kept close to the test samples. Table 1 summarizes the average strength of cylinders tested on the same day of testing. Steel bars considered in this study have a commercial yield strength and a modulus of elasticity of 400 MPa and 200 GPa, respectively. The headed-end and straight bars used in specimens S2, S3, S4, S5 and S6 were ribbed-surface GFRP bars with 1188-MPa tensile strength and 60-GPa modulus of elasticity.



(a) Closure strip for slab S3



(b) Closure strip for slab S4



(c) Closure strip for slab S5



(d) Closure strip for slab S6

Fig. 6 Views of closure strip in jointed slabs

The structural response during the static loading of the specimens was captured through the use of electronic instrumentation. Potentiometers and Linear variable differential transducers (LVDTs) were used to measure deflections at mid-span of the slab specimens. A static patch load, simulating CHBDC truck wheel load was applied to examine the structural behavior and ultimate load carrying capacity of the proposed connection details as compared to the control cast-in-place slabs S1 and S2 reinforced with steel and GFRP bars, respectively. All slabs were tested under a 250x600 mm single patch load at the center of their clear span. This patch load is equivalent to the foot print of CHBDC wheel load of 87.5 kN. The slab ends were simply-supported over roller support at one end and hinged support at the other end. Figure 7 shows the experimental setup used for testing the deck slab samples. As depicted in Fig. 7. The 600-mm length of the wheel load was divided into two segments, one from each side of the mid-span using two steel plates of 250 mm length each and 100 mm gap between them to allow for steel plate rotation at the mid-span with load increase. To conduct static

load tests to-collapse, the jacking load was applied in increments to allow for observing the behavior of the specimen visually and to mark cracks. The available data acquisition system 5000 was used to capture readings from sensors as well as the load cell located between the jacking piston and the top of the deck slab. After every load increment, start of tension cracks and crack propagations were monitored. It should be noted that incremental loading technique was considered during testing on which the specimen was loaded to 10 kN, followed by load release. Then, the specimen was loaded to 20 kN, followed by load release. These incremental loading steps were repeated with a total load increase of 10 kN in each step till the specimen failed. The following section discusses the structural behavior of the test specimens.

Table 1. Summary of slab configurations and test results

Slab	Reinforcement	Slab type	f'_c MPa		Cracking load (kN)	Ultimate load (kN)	Ultimate Deflection (mm)
			Concrete	Grout/UHPC			
S1	Steel straight bars (3-10mm)	Cast-in-place	38.3	-	30	95	99
S2	GFRP straight bars (4-16mm)	Cast-in-place	41.36	-	30	165.74	38.7
S3	GFRP straight bars (4-16mm)	Precast with 300 mm closure strip filled with NSG [§]	57.76	63.05	10	80.76	15.2
S4	GFRP headed bars (4-16mm)	Precast with 200 mm closure strip filled with NSG [§]	65.03	68.76	16	80.54	14.33
S5	GFRP headed bars (3-16mm)	Precast with trapezoidal-shaped closure strip filled with NSG [§]	57.76	62.84	15	67.99	16.57
S6	GFRP headed bars (4-16mm)	Precast with 125 mm closure strip filled with UHPC [*]	56.36	159.83	20	120.42	25.1

[§]NSG = non-shrink grout; ^{*}UHPC = ultra-high performance concrete

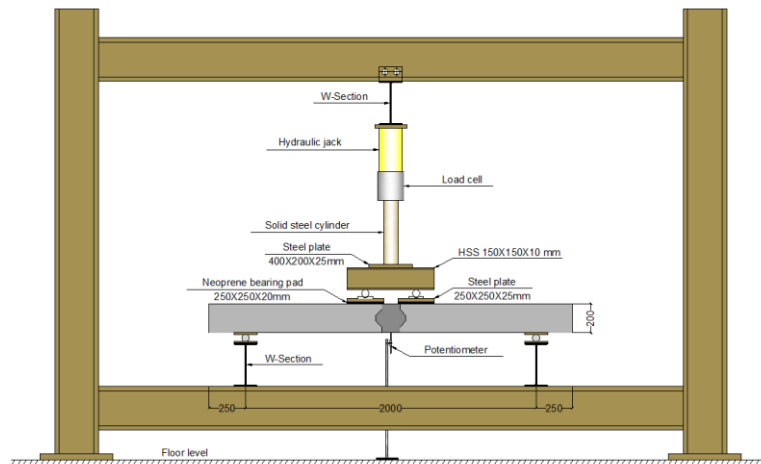


Fig. 7 Test setup

TEST RESULTS

This section discusses the structural behavior of the tested specimens in the form of crack pattern, bar condition at failure, slab deflection and ultimate load carrying capacity. Figure 8 shows the crack pattern at failure at the side of the slab for the cast-in-place slab S1 with reinforcing steel bars. It was observed that the first visual flexural crack appeared at the bottom of the slab at the mid-span location at a load of 30 kN. Other flexural cracks appeared within the quarter points of the span and propagated towards the top surface of the slab with increase in load till failure. Crushing of concrete at the top surface of the slab at the mid-span location was observed at the maximum jacking load of 95 kN and slab deflection of 99 mm, leading to pure flexural flexure.

Figure 9 shows the crack pattern at failure of cast-in-place slab S2 with GFRP bars. It was observed that the first visible flexural crack appeared at a load of 30 kN. Other flexural crack appeared at higher load increments and spread over a length greater than that for slab S1. A diagonal shear crack suddenly appeared between the load location and quarter point location that widened and propagated to the vicinity of the applied load location and the support causing concrete crushing at the top surface of slab, as shown in Fig. 9-a, leading to slab collapse. Failure occurred at an ultimate load of 166 kN and deflection of 38.7 mm due to combined shear and bending. By comparing the ultimate load capacity of slabs S1 and S2, it can be observed that the GFRP-reinforced slab exhibited a flexural strength about 75% greater than that for a similar slab reinforced with steel bars. It should be noted that both slabs were reinforced per the reinforcement ratios specified in CHBDC.



(a) Side view



(b) Bottom view

Fig. 8 Crack behavior for deck slab S1



(a) Side view



(b) Bottom view

Fig. 9 Crack behavior for deck slab S2

Figure 10 shows the crack pattern at failure of precast slab S3 with 300-mm wide closure strip and projected bottom straight GFRP bars. It was observed that the first hairline cracks were formed at the cold joint between the precast concrete and the closure strip at a load of 10 kN. These fine cracks started to widen gradually with increase in applied load. Several flexural cracks appeared in the precast slab closer to the closure strip as depicted in Fig. 10-a. Prior to failure, set of deep longitudinal and transverse cracks propagated along the underside of the cold joint followed by development of a wide flexural crack at both sides of the cold joint as shown in Fig. 10-b. Failure of slab S3 at 80.8-kN ultimate load and 15-mm deflection was due to loss of bond combined with slippage of GFRP bars from the cold joint as depicted in Fig. 14-a.



Fig. 10 Crack behavior for deck slab S3

Figure 11 shows the crack pattern at failure of precast slab S4 with 200-mm wide closure strip and projected bottom headed-end GFRP bars. It was noticed that the first hairline cracks were formed at the cold joint between the precast concrete and the closure strip at a load of 16 kN. These fine cracks started to widen gradually with increase in applied load. Few flexural cracks appeared in the precast slab closer to the closure strip as depicted in Fig. 11-a. Close to failure, a wide transverse cracks propagated along the underside of the cold joint indicating a loss of bond, followed by propagation of a wide flexural crack at both sides of the cold joint as shown in Fig. 11. Failure of slab S4 at 80.5-kN ultimate load and 14-mm deflection was due to loss of bond combined with breakage of the bar head within the closure strip as shown in Fig. 14-b. It can be observed that slab S3 and S4 are not considered as good as the steel-reinforced slab S1 for ultimate strength since their ultimate capacities are 15% less than that for slab S1.

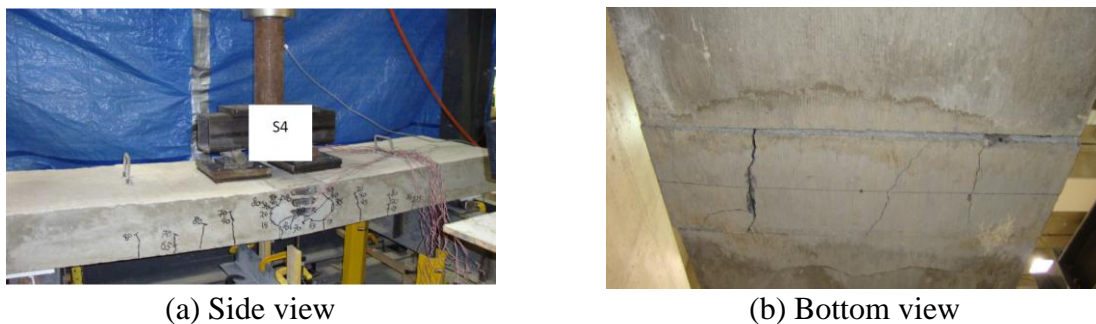


Fig. 11 Crack behavior for deck slab S4

Figure 12 shows the crack pattern at failure of precast slab S5 with 100-mm wide closure strip and staggered 100-mm wide trapezoidal-shaped interlock, and projected bottom headed GFRP bars. It was noticed that the first hairline cracks were formed at the cold joint between the precast concrete and the closure strip at a load of 15 kN. These fine cracks started to widen gradually with increase in applied load. Few flexural cracks appeared in the precast slab closer to the closure strip as shown in Fig. 12-a. Prior to failure, large longitudinal and transverse cracks propagated along the underside of the cold joint followed by formation of a wide diagonal flexural crack at both sides of the cold joint as depicted in Fig. 12. Failure of slab S5 at 68-kN ultimate load and 17-mm deflection was due to loss of bond combined with breakage of the bar head as shown in Fig. 14-c. Given the fact that this specimen has 3 main bars in the tension side in contrast to 4 bars in other GFRP-reinforced slab, the ultimate load can be approximated as $67.99 \times (4/3) = 90.65$ kN which is still less than that for the steel-reinforced slab S1. As such, it can be concluded that slab S5 is not considered as good as the steel-reinforced slab S1 with respect to ultimate strength.



Fig. 12 Crack behavior for deck slab S5

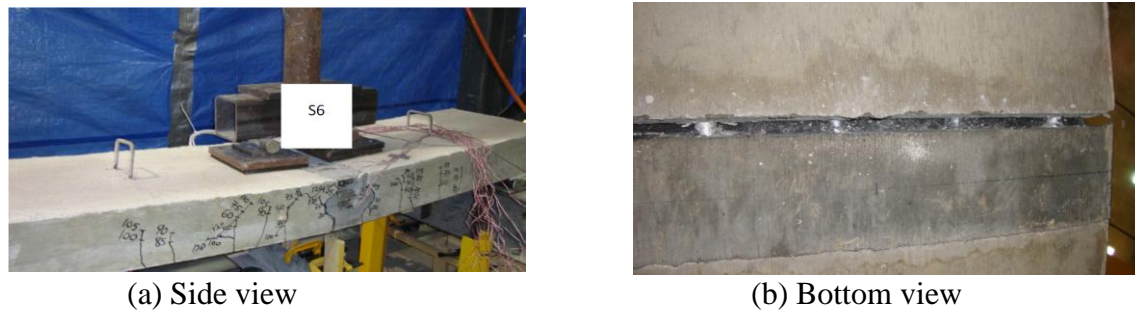


Fig. 13 Crack behavior for deck slab S6

Figure 13 shows the crack pattern at failure of the precast slab S6 with 125-mm wide closure strip and projected bottom headed-end GFRP bars embedded in UHPC. It was observed that the first hairline cracks were formed at the cold joint between the precast concrete and the closure strip at a load of 20 kN. These fine cracks started to widen gradually as the loading increased. Few flexural cracks appeared in the precast slab closer to the closure strip as shown in Fig. 13-a. Prior to failure, a wide flexural crack propagated along the underside of the cold joint between the precast concrete and the closure strip as shown in Fig. 13-b. In addition, slight slippage of bar from the headed-end outer disk was observed as shown in Fig. 14-e. This type of deformation was observed after taking a core sample of the joint and

slicing it using saw-cutting. As such, failure of slab S6 was due to slippage of the bars from head within the closure strip combined with crushing of top surface concrete at 120.4-kN ultimate load and 25.1-mm deflection. It can be noted that slab S6 is considered as good as the steel-reinforced slab S1 since its ultimate capacity is 27% greater than that for slab S1.



(a) Bar debonding in slab S3



(b) Bar head breakage in slab S4



(c) Bar shear breakage in slab S5



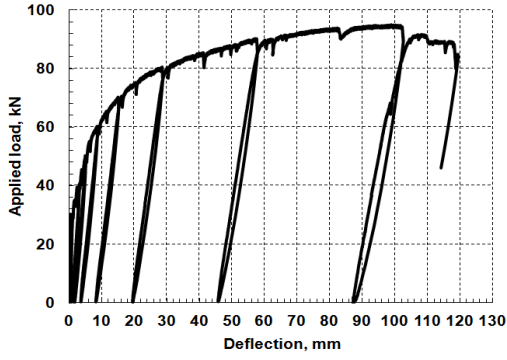
(d) Concrete crushing in slab S6



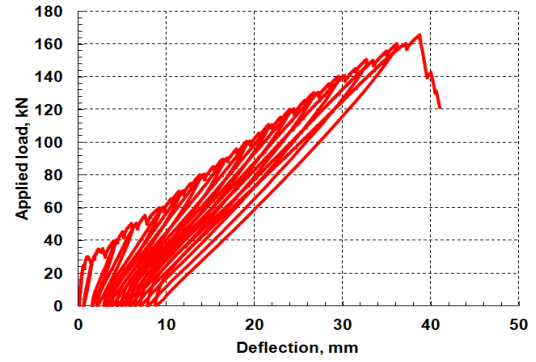
(e) Bar slippage from the head in slab S6

Fig. 14 Selected failure types in GFRP-reinforced slabs

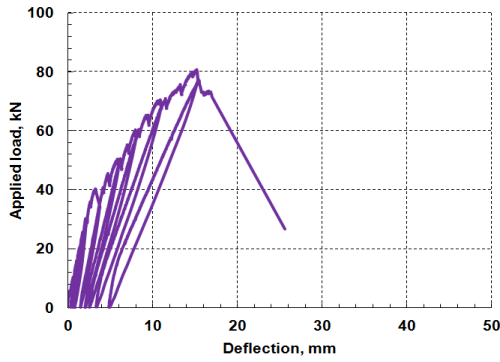
Figure 15 depicts the incremental load-deflection history of all tested specimens. While Fig. 16 shows comparison between the load-deflection relationship of the tested specimens using the envelope of all phases of incremental loading. It can be observed that maximum deflection at failure of the best GFRP-reinforced jointed slab S6 was 25.1 mm compared to 99 mm in case of reinforced-steel cast-in-place slab S1. In addition, the failure load of slab S6 is 120.42 kN compared to 95 kN for slab S1. As such, it can be concluded that jointed slab S6 with closure strip filled with UHPC has the best joint among other proposed joints and that it was proved as good as the CHBDC-specified steel-reinforced cast-in-place slab with respect to ultimate and serviceability limit state requirements.



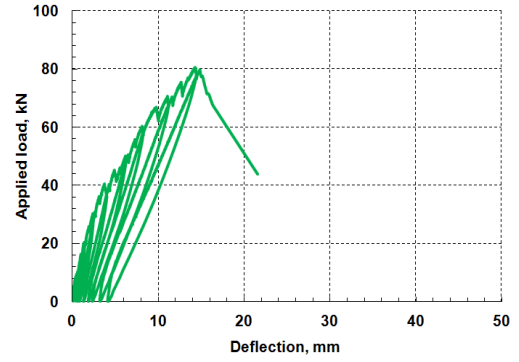
(a) Slab S1



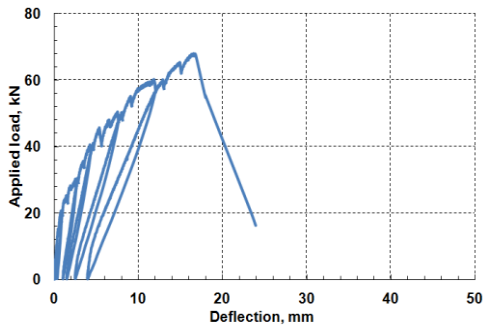
(b) Slab S2



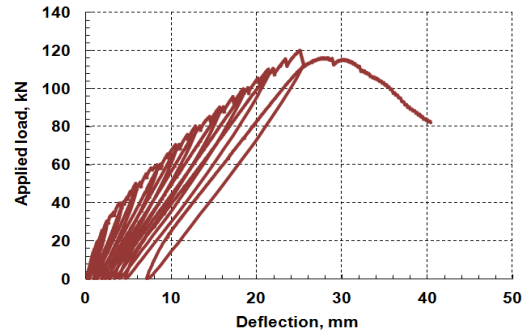
(c) Slab S3



(d) Slab S4



(e) Slab S5



(f) Slab S6

Fig. 15 Load-deflection relationships obtained at mid-span of slab specimens

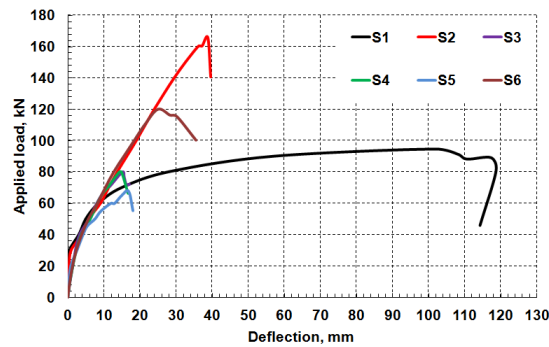


Fig. 16 Load-deflection relationships obtained at mid-span of all slab specimens

CONCLUSIONS

This paper investigates the use of GFRP bars in cast-in-place bridge deck slabs as well as precast bridge deck slab of prefabricated bridge girders to determine their structural behavior and ultimate load carrying capacities when subjected to CHBDC wheel loading. The results were correlated to a control slab reinforced with steel bars. Based on the experimental results, it can be concluded that for cast-in-place slabs reinforced with the reinforcement ratio specified in CHBDC, the ultimate load capacity of GFRP-reinforced cast-in-place slab is about 75% greater than that for a similar slab reinforced with steel bars. Also, it can be concluded that the 125-mm wide closure strip with projecting headed-end GFRP bars filled with UHPC has a load carrying capacity about 27% greater than that for a similar slab reinforced with steel bars. Such joint proved to be the best among other proposed joints filled with non-shrink grout. Further tests are currently conducted to examine the fatigue life of the successful control joints under simulated vehicular wheel loading.

ACKNOWLEDGMENTS

The authors would also like to acknowledge the support of Ontario Centers of Excellence's Collaborative Research fund, and Schoeck Canada Inc. The authors would like to thank Euclid Chemical Company for supplying grout material and Lafarge North America Inc. for supplying the UHPC mix.

REFERENCES

- 1- CHBDC. 2006. Canadian Highway Bridge Design Code, CAN/CSA-S6-06. Canadian Standard Association, Toronto, Ontario, Canada.
- 2- AASHTO. 2010. AASHTO-LRFD Bridge Design Specifications. American Association of State Highway and Transportation Officials, Washington, DC.
- 3- Shah, K. Sennah, R. Kianoush, Siyin Tu and Clifford Lam. 2006. Flange-to-Flange Moment Connections for Precast Concrete Deck Bulb-Tee Bridge Girders. *Journal of Prestressed Concrete Institute, PCI*, 51(6): 86-107.
- 4- Shah, B., Sennah, K., Kianoush, R., Tu, S. and Lam, C. 2007. Experimental Study on Prefabricated Concrete Bridge Girder-to-Girder Intermittent-Bolted Connection Systems. *ASCE journal of Bridge Engineering*, 12(5): 570-584.
- 5- Au, A., Lam, C., and Tharmabala, B. 2008. Investigation of Prefabricated Bridge Systems using Reduced-Scale Models, *PCI Journal*, 53(6): 67-95.
- 6- Au, A., Lam, C., and Tharmabala, B. 2011. Investigation of Closure Strip Details for Connecting Prefabricated Deck Systems, *PCI Journal*, 56(3): 75-93.
- 7- www.schoeck-canada.com.